Journal of Southeast University (English Edition) Vol. 23, No. 1, pp. 75 – 80 Mar. 2007 ISSN 1003—7985

Numerical simulation of concrete shrinkage based on heat and moisture transfer in porous medium

Chen Depeng Qian Chunxiang

(School of Materials Science and Engineering, Southeast University, Nanjing 211189, China)

Abstract: To simulate the concrete shrinkage in varying temperature and moisture environments, a simulate procedure comprising an analytical process and a finite element analysis is proposed based on the coupled partial differential equations describing heat and moisture transfer in a porous medium. Using the Laplace transformation method and transfer function to simplify and solve the coupled equations in Laplace domain, the moisture and temperature distribution in time domain are obtained by inverse Laplace transformation. The shrinkage deformations of concrete are numerically simulated by the finite element method (FEM) based on the obtained temperature and moisture distribution. This approach avoids the complex eigenvalues, coupling difficulty and low accuracy found in other solving methods, and also effectively calculates the moisture induced shrinkage which is almost impossible using familiar FEM software. The validity of the simulation procedure is verified by Hundt's test data. The results reveal that the proposed approach can be considered a reliable and efficient method to simulate the coupling moisture and temperature shrinkage of concrete.

Key words: coupling heat-moisture transfer; concrete shrinkage; analytical method; transfer function

Concrete shrinkage due to temperature and moisture conditions will develop simultaneously under normal conditions. Some properties of concrete, such as thermal conductivity, specific heat capacity, and even elastic modulus, are affected by moisture variations. Similarly, moisture diffusivity and surface water evaporation will fluctuate with moisture conditions. Nevertheless, it would be more practical to study the volume stability of concrete using a coupled temperature and moisture model, provided this model concept would lead to accurate predictions of the deformations in the concrete structure under actual environmental conditions.

Luikov has proposed the governing equations for coupling heat and mass transfer in porous materials. Quite a few researchers have given different solution methods. Mikhailov and Ozisik had given the analytical solutions based on the classical integral transform method[1]. Gaur and Bansal used the periodic approximate method to obtain closed-form solutions[2]. Chang and Chen applied a decoupling technique to coupled governing equations[3]. Cheroto et al. proposed a modified lumped system analysis approach to get approximate solutions[4]. But the methods referred to are either complicated or incorrect[3,5]. The modified Luikov equations and the transfer function are applicable to simulate the temperature and moisture distribution in a concrete[3].

In this paper, the thermal-drying shrinkage of concrete is simulated by means of the analytical method and the FEM method based on the coupled heat-moisture transfer equations in a porous medium.

1 Coupling Heat-Moisture Transfer Equations

1.1 Theoretical framework

Material properties are considered to be uniform throughout the material body. The requirements of mass and energy conservation during the transfer process lead to the following partial differential equations:

$$\rho c_{\mathrm{p}} \frac{\partial T}{\partial t} = \lambda \frac{\partial^2 T}{\partial x^2} + \rho r h_{\mathrm{lv}} \frac{\partial M}{\partial t} \tag{1}$$

$$\frac{\partial M}{\partial t} = D_{\mathrm{m}} \frac{\partial^2 M}{\partial x^2} + D_{\mathrm{m}} \delta \frac{\partial^2 T}{\partial x^2} \tag{2}$$

where ρ is the density of the material, c_{p} is the specific heat of constituent, T is the temperature, λ is the thermal conductivity, r is the phase change factor, M is the moisture content, h_{lv} is the heat of phase change, D_{m} is the moisture diffusion coefficient, and δ is the thermal gradient coefficient.

Eqs. (1) and (2) express the energy and mass conservation requirements, respectively. This can be

Received 2006-09-26.

Foundation items: The National Natural Science Foundation of China (No. 50539040), the Trans-Century Training Programme Foundation for the Talents by the State Education Commission (No. NCET-05-0473).

Biographies: Chen Depeng (1978—), male, graduate; Qian Chunxiang (corresponding author), female, doctor, professor, cxqian@seu.edu.cn.

simplified into

$$L\frac{\partial^2 T}{\partial x^2}=\frac{\partial T}{\partial t}-v\frac{\partial M}{\partial t} \tag{3}$$

$$D\frac{\partial^2 M}{\partial x^2}=\frac{\partial M}{\partial t}-\theta\frac{\partial T}{\partial t} \tag{4}$$

where $L=\lambda/(\rho c_p)$, $v=rh_{lv}/c_p$, $\theta=\rho c_p D_m\delta/(\lambda+\rho D_m\delta rh_{lv})$, and $D=\lambda D_m/(\lambda+\rho D_m\delta rh_{lv})$.

Eqs. (3) and (4) describe the joint time-dependent heat-moisture coupling transfer process. Fig. 1 is the schematic diagram of a concrete specimen, the thermal-drying shrinkage of which will be studied in this paper.

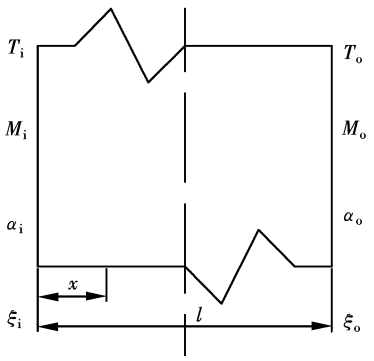

Fig. 1 Schematic diagram of the concrete specimen

1.2 Boundary conditions

At the boundaries of the domain, the heat of phase change becomes a part of the energy balance, and the mass diffusion caused by the temperature and moisture gradients affects the mass balance. The associated hygro-thermal boundary and initial conditions can be given as[3]

$$\lambda\left.\frac{\partial T(x,t)}{\partial x}\right|_{x=0}=\alpha_i[T(0,t)-T_i]+(1-p)h_{lv}\zeta_i[M(0,t)-M_i] \tag{5}$$

$$\lambda\left.\frac{\partial T(x,t)}{\partial x}\right|_{x=l}=\alpha_o[T(l,t)-T_o]+(1-p)h_{lv}\zeta_o[M(l,t)-M_o] \tag{6}$$

$$D_m\left.\frac{\partial M(x,t)}{\partial x}\right|_{x=0}+D_m\delta\left.\frac{\partial T(x,t)}{\partial x}\right|_{x=0}=\zeta_i[M(0,t)-M_i] \tag{7}$$

$$D_m\left.\frac{\partial M(x,t)}{\partial x}\right|_{x=l}+D_m\delta\left.\frac{\partial T(x,t)}{\partial x}\right|_{x=l}=\zeta_o[M(l,t)-M_o] \tag{8}$$

where α is the heat transfer coefficient, p is the ratio of vapor diffusion coefficient to coefficient of total moisture diffusion (evaporation number), ζ is the moisture transfer coefficient, and the subscripts i and o indicate the inner and exterior surfaces, respectively. Eqs. (5) and (6) represent the heat flux in terms of convection heat transfer and phase-change energy transfer, expressing the heat equilibrium at internal and exterior surfaces. Eqs. (7) and (8) represent the moisture balance at the two surfaces.

The initial temperature and moisture values in concrete are given by

$$T(x,0)=T_0 \tag{9}$$

$$M(x,0)=M_0 \tag{10}$$

2 Solution Procedure

The complete procedure for the numerical simulation of concrete deformations consists of three steps. First, the coupled temperature and moisture distribution is determined. Secondly, the stress induced by moisture distribution is calculated by relevant equations. Finally, the thermal-drying shrinkage of concrete resulting from the moisture and heat gradient is computed.

2.1 Temperature and moisture distribution

Laplace transformation on time variable t is applied to Eqs. (3) to (10). Consequently, the corresponding equations become

$$L\frac{\mathrm{d}^2\bar{T}}{\mathrm{d}x^2}=s\bar{T}-T_0-vs\bar{M}+vM_0 \tag{11}$$

$$L\frac{\mathrm{d}^2\bar{M}}{\mathrm{d}x^2}=s\bar{M}-M_0-\theta s\bar{T}+\theta T_0 \tag{12}$$

$$\lambda\left.\frac{\mathrm{d}\bar{T}(x,s)}{\partial x}\right|_{x=0}=\alpha_i\left[\bar{T}(0,s)-\frac{\bar{T}_i}{s}\right]+(1-\varepsilon)h_{lv}\zeta_i\left[\bar{M}(0,s)-\frac{M_i}{s}\right] \tag{13}$$

$$-\lambda\left.\frac{\mathrm{d}\bar{T}(x,s)}{\partial x}\right|_{x=l}=\alpha_o\left[\bar{T}(l,s)-\frac{\bar{T}_o}{s}\right]+(1-\varepsilon)h_{lv}\zeta_o\left[\bar{M}(l,s)-\frac{\bar{M}_o}{s}\right] \tag{14}$$

$$D_m\left.\frac{\mathrm{d}\bar{M}(x,s)}{\partial x}\right|_{x=0}+D_m\delta\left.\frac{\mathrm{d}\bar{T}(x,s)}{\partial x}\right|_{x=0}=\zeta_i\left[\bar{M}(0,s)-\frac{\bar{M}_i}{s}\right] \tag{15}$$

$$-D_m\left.\frac{\mathrm{d}\bar{M}(x,s)}{\partial x}\right|_{x=l}-D_m\delta\left.\frac{\mathrm{d}\bar{T}(x,s)}{\partial x}\right|_{x=l}=\zeta_o\left[\bar{M}(l,s)-\frac{\bar{M}_o}{s}\right] \tag{16}$$

$$\bar{T}(x,0)=\frac{T_0}{s} \tag{17}$$

$$\bar{M}(x,0)=\frac{M_0}{s} \tag{18}$$

where s is the Laplace transformation parameter.

Next, a transfer function $\varphi(x,s)$ is introduced that satisfies

$$\bar{T}(x,s)=\frac{v}{L}\varphi(x,s)+\frac{T_0}{s} \tag{19}$$

$$\bar{M}(x,s)=\frac{1}{L}\varphi(x,s)-\frac{1}{s}\frac{\mathrm{d}^2\varphi(x,s)}{\mathrm{d}x^2}+\frac{M_0}{s} \tag{20}$$

Consequently, Eq. (11) is satisfied, while Eq. (12) becomes

$$\frac{\mathrm{d}^4\varphi}{\mathrm{d}x^4}-\frac{s}{D}\left(1+\frac{D}{L}\right)\frac{\mathrm{d}^2\varphi}{\mathrm{d}x^2}+\frac{s^2(1-v\theta)}{LD}\varphi=0 \quad (21)$$

Thus, the heat and moisture transfer coupling differential equations are transformed into a single fourth-order ODE (Eq. (21)), which can readily be solved.

Assume that $\varphi(x, s)$ has the following form

$$\varphi(x, s) = \sum_{i=1}^{4}\zeta_i(s)\,s^{p_i x} \quad (22)$$

where

$$p_i=\sqrt{s}q_i$$

$$q_i=\frac{a_i}{\sqrt{2D}}\left[1+\frac{D}{L}+b_i\sqrt{\left(1-\frac{D}{L}\right)^2+\frac{4\theta vD}{L}}\right]^{\frac{1}{2}}$$

$$a_i=\begin{cases}-1 & i=1,2\\ 1 & i=3,4\end{cases}$$

$$b_i=\begin{cases}-1 & i=1,3\\ 1 & i=2,4\end{cases}$$

Obviously, $q_3=-q_1$ and $q_4=-q_2$.

The coefficients $\zeta_i(s)$ ($i=1, 2, 3, 4$) are determined by Eqs. (13) to (16), and can be written as

$$\boldsymbol{K}\zeta(s)=\boldsymbol{Q} \quad (23)$$

When the boundary conditions are defined as $T(0, t)=T_\mathrm{i}$, $T(l, t)=T_\mathrm{o}$, $M(0, t)=M_\mathrm{i}$, $M(l, t)=M_\mathrm{o}$, $\boldsymbol{K}$ and $\boldsymbol{Q}$ can be expressed as

$$\boldsymbol{K}=\begin{bmatrix}\frac{v}{L} & \frac{v}{L} & \frac{v}{L} & \frac{v}{L}\\ \frac{v}{L}\mathrm{e}^{p_1 l} & \frac{v}{L}\mathrm{e}^{-p_1 l} & \frac{v}{L}\mathrm{e}^{p_1 l} & \frac{v}{L}\mathrm{e}^{-p_1 l}\\ \frac{1}{L}-q_1^2 & \frac{1}{L}-q_2^2 & \frac{1}{L}-q_1^2 & \frac{1}{L}-q_2^2\\ \left(\frac{1}{L}-q_1^2\right)\mathrm{e}^{p_1 l} & \left(\frac{1}{L}-q_2^2\right)\mathrm{e}^{-p_1 l} & \left(\frac{1}{L}-q_1^2\right)\mathrm{e}^{p_1 l} & \left(\frac{1}{L}-q_2^2\right)\mathrm{e}^{-p_1 l}\end{bmatrix} \quad (24)$$

$$\boldsymbol{Q}=\begin{bmatrix}\frac{T_\mathrm{i}-T_0}{s} & \frac{T_\mathrm{o}-T_0}{s} & \frac{M_\mathrm{i}-M_0}{s} & \frac{M_\mathrm{o}-M_0}{s}\end{bmatrix}^{\mathrm{T}} \quad (25)$$

The solution of Eq. (23) can be determined by Cramer's rule, and is expressed as

$$\zeta_k(s)=\begin{cases}\dfrac{n_k+m_k\mathrm{e}^{-\frac{q_k}{\sqrt{s}}}}{s(\mathrm{e}^{\frac{q_k}{\sqrt{s}}}-\mathrm{e}^{-\frac{q_k}{\sqrt{s}}})} & k=1,2\\ -\dfrac{n_j+m_j\mathrm{e}^{-\frac{q_j}{\sqrt{s}}}}{s(\mathrm{e}^{\frac{q_j}{\sqrt{s}}}-\mathrm{e}^{-\frac{q_j}{\sqrt{s}}})} & k=3,4;\ j=k-2\end{cases} \quad (26)$$

where

$$n_1=\frac{(M_\mathrm{o}-M_0)v-(1-Lq_2^2)(T_\mathrm{o}-T_0)}{L(q_2^2-q_1^2)}$$

$$n_2=-\frac{(M_\mathrm{o}-M_0)v-(1-Lq_1^2)(T_\mathrm{o}-T_0)}{L(q_2^2-q_1^2)}$$

$$m_1=\frac{(M_i-M_0)v-(1-Lq_2^2)(T_i-T_0)}{L(q_2^2-q_1^2)}$$

$$m_2=-\frac{(M_i-M_0)v-(1-Lq_1^2)(T_i-T_0)}{L(q_2^2-q_1^2)}$$

The temperature and moisture solutions of Eqs. (19) and (20) are obtained in the Laplace domain. They can be formulated as

$$\overline{T}(x, s)=\frac{v}{L}\sum_{i=1}^{2}\frac{A_i\mathrm{sh}(q_i x\sqrt{s})+B_i\mathrm{sh}(q_i(x-l)\sqrt{s})}{s\mathrm{sh}(q_i l\sqrt{s})}+\frac{T_0}{s} \quad (27)$$

$$\overline{M}(x, s)=\sum_{i=1}^{2}\left(\frac{1}{L}-q_i^2\right)\cdot\frac{A_i\mathrm{sh}(q_i x\sqrt{s})+B_i\mathrm{sh}(q_i(x-l)\sqrt{s})}{s\mathrm{sh}(q_i l\sqrt{s})}+\frac{M_0}{s} \quad (28)$$

Next, applying inverse Laplace transformation to Eqs. (27) and (28) yields the temperature and moisture solution in time and space domains. They can be expressed as

$$T(x, t)=\sum_{i=1}^{4}\sum_{j=1}^{2}\frac{Q_{ij}}{2q_j l}\cdot\left[2\sqrt{\frac{t}{\pi}}\exp\left(-\frac{n_{ij}^2}{4t}\right)-n_{ij}\mathrm{erfc}\left(\frac{n_{ij}}{2\sqrt{t}}\right)\right]+T_0 \quad (29)$$

$$M(x, t)=\sum_{i=1}^{4}\sum_{j=1}^{2}\left(\frac{1}{L}-q_i^2\right)\frac{Q_{ij}}{2q_j l}\cdot\left[2\sqrt{\frac{t}{\pi}}\exp\left(-\frac{n_{ij}^2}{4t}\right)-n_{ij}\mathrm{erfc}\left(\frac{n_{ij}}{2\sqrt{t}}\right)\right]+M_0 \quad (30)$$

where

$$n_{ij}=\begin{cases}q_i(jl-x) & i=1,2;\ j=1,2\\ q_{i-2}((j-1)l+x) & i=3,4;\ j=1,2\end{cases}$$

$$\mathrm{erfc}(x)=\int_x^\infty \mathrm{e}^{-t^2}\mathrm{d}t$$

$$\boldsymbol{Q}_{ij}=\begin{bmatrix}n_1 & m_1\\ n_2 & m_2\\ -m_1 & -n_1\\ -m_2 & -n_2\end{bmatrix}$$

2.2 Moisture distribution induced stress

The deformations induced by temperature changes can be calculated by direct application of temperature loads to the nodes in the FE analysis. On the contrary, with the current FEM approach it is impossible to directly apply moisture loads to the nodes.

Drying shrinkage is induced by moisture loss from the pore structure after the concrete has attained final set through evaporation and diffusion. According to the Kelvin-Laplace equation, there exists a relationship between the negative pore fluid pressure and the

internal relative humidity within the pore structure, which can be expressed as

$$\sigma = \frac{-\ln(H_r)}{v_m} RT \tag{31}$$

where σ is the negative pore fluid pressure, H_r is the internal relative humidity, R is the universal gas constant, T is the temperature, and v_m is the molar volume of water.

A relationship between the hydrostatic pressure and the associated strain is proposed by Mackenzie[6-7]. It can be expressed as

$$\varepsilon = p_a\left(\frac{1}{3K} - \frac{1}{3K_0}\right) \tag{32}$$

where ε is the linear strain, p_a is the average hydrostatic pressure (i. e., equal to σ from the Kelvin-Laplace equation), K is the bulk modulus of porous solid, and K_0 is the bulk modulus of the solid skeleton of the material. When Eq. (32) is used for a partially saturated porous medium like concrete, it should be multiplied by a saturation factor[6]. Concrete is a composite material in which the aggregate is volume stable; its grains restrain the shrinkage of the cement paste. Eq. (32) has been modified again[6], therefore, to account for the volume fraction of aggregate

$$\varepsilon = pS\left(\frac{1}{3K} - \frac{1}{3K_0}\right)\frac{V_p}{V_c} \tag{33}$$

where S is the saturation factor, and V_p/V_c is the volume fraction of the paste in the concrete. The bulk modulus for a porous medium such as concrete is governed by the porosity and the elastic moduli of the concrete[7], namely c, K_0 and G_0, whereby G_0 and c are the shear modulus and porosity, respectively. So,

$$\frac{K}{K_0} = 1 - \frac{c(3K_0 + 4G_0)}{4G_0} \tag{34}$$

The stress on each node can be imagined as the arithmetic product of strain and elastic modulus. Consequently, the stress induced by moisture changes can be calculated by

$$\sigma_h = \frac{4G_0^2 S}{4G_0(1-c) + 3K_0} \frac{-\ln H_r}{3K_0 v_m} RT \frac{V_p}{V_c} \tag{35}$$

2.3 Concrete shrinkage

Once the temperature and moisture loads have been applied to the element's nodes, the shrinkage deformation of concrete can be numerically simulated by the FEM method.

3 Case Analysis

3.1 Brief introduction of Hundt's test

In order to validate the applicability of the present simulation procedure in predicting the coupled heat and moisture transfer in concrete and the induced thermal-drying shrinkage of concrete, we applied the method to a test case which was carried out by Hundt[8]. Hundt investigated different transport phenomena in six concrete specimens over a time period of three years, and the experimental results are suitable to as benchmarks in verifying the validity of numerical models. In the experiment, a prismatic concrete specimen of a size of 2.4 m × 0.4 m × 0.4 m was used and the concrete was cured for 28 d before test. The specimen was isolated with regards to thermal as well as moisture flux along the surfaces situated alongside to simulate 1D-conditions (see Fig. 2). It was subjected to a temperature of 80 ℃ at one end and to a rapid decrease of external relative humidity (45%) at the other end.

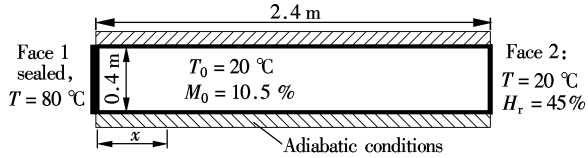

Fig. 2 Schematic of layout and boundary conditions of Hundt's test on a concrete specimen

At an internal relative humidity below approximately 45%, capillary menisci are not stable and the Kelvin-Laplace equation is not reasonable for expressing the moisture induced stress. While in Hundt's test, even though air relative humidity is 45%, the relative humidity inside the concrete rarely drops below 50%[9]. Therefore, it is obvious that the simulation procedure is applicable in this case.

3.2 Comparison of numerical results and Hundt's test data

According to Eqs. (5) to (10), the boundary conditions in this case are expressed as Eqs. (36) to (39). The initial conditions and some basic parameters are $l = 2.40$, $T_0 = 20$ ℃, $M_0 = 10.5$, $T_i = 80$ ℃, $T_o = 20$ ℃, $M_o = 3.5\%$ (calculated from $H_r = 45\%$). In the simulation analysis, the concrete specimen is discretized by 8-nodes block elements and a constant time step of 12 h is used.

$$\lambda \left.\frac{\partial T(x,t)}{\partial x}\right|_{x=0} = \alpha_i[T(0,t) - T_i] \tag{36}$$

$$\lambda \left.\frac{\partial T(x,t)}{\partial x}\right|_{x=l} = \alpha_o[T(l,t) - T_o] + (1-p)h_{lv}\zeta_o[M(l,t) - M_o] \tag{37}$$

$$D_m \left.\frac{\partial M(x,t)}{\partial x}\right|_{x=0} + D_m\delta \left.\frac{\partial T(x,t)}{\partial x}\right|_{x=0} = 0 \tag{38}$$

$$D_m \left.\frac{\partial M(x,t)}{\partial x}\right|_{x=l} + D_m\delta \left.\frac{\partial T(x,t)}{\partial x}\right|_{x=l} = \zeta_o[M(l,t) - M_o] \tag{39}$$

The numerical results are compared with the experimental data of Hundt's test between the moisture content (volume ratio), the temperature and the length changing of the specimen (see Figs. 3 to 5). It should be noted that the simulated moisture distribution is the mass content of moisture directly from the analytic solution of heat and moisture transfer equations according to the boundary conditions. In order to compare the numerical results to Hundt's test data, the numerical results of mass content were changed into volume content before comparison with the experimental results of Hundt's test.

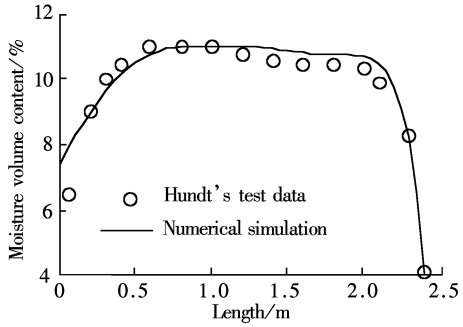

Fig. 3 Comparison of numerical and experimental moisture distribution

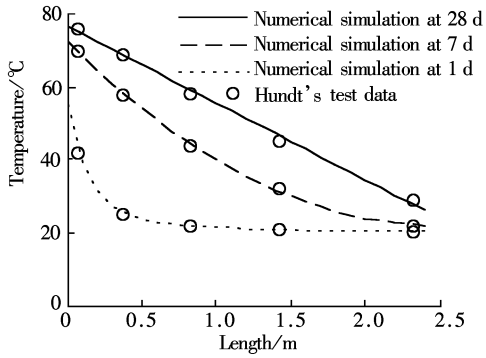

Fig. 4 Comparison of numerical and experimental temperature distribution

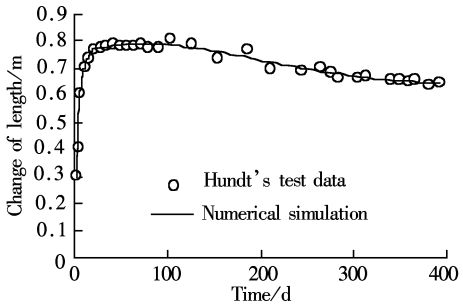

Fig. 5 Comparison of numerical and experimental length changing of the specimen within the first 400 d

Obviously, Figs. 3 to 5 show a relatively good correlation between numerical and experimental data. The simulation procedure proposed in this paper is reliable and suitable for thermal-drying shrinkage simulation of concrete.

4 Conclusion

The simulation procedure proposed in this paper is based on the coupling of heat and moisture transfer effects in porous concrete. It encompasses an analytical solution of temperature and moisture distribution in concrete, a numerical simulation of the stress fields induced by moisture and heat distribution, and the mathematical computation of thermal-drying shrinkage deformation in concrete specimens. The validity of the method of analysis was verified by comparing Hundt's test data with its analytical results. The results reveal the rationality and efficiency of the coupling model and the simulation process.

The heat and moisture transfer inside porous materials such as concrete is a complex phenomenon. More theoretical investigations are needed to be carried out for more insight into the variation of the heat and moisture transfer for different types of concrete and in various environmental conditions.

Acknowledgement We would like to thank Prof. Piet Stroeven and Guo Zhanqi at Delft University of Technology for their suggestions on revising this paper.

References

[1] Pandey R N, Srivastava S K, Mikhailov M D. Solutions of Luikov equations of heat and mass transfer in capillary porous bodies through matrix calculus: a new approach [J]. *International Journal of Heat and Mass Transfer*, 1999, **42**(14): 2649 – 2660.

[2] Gaur R C, Bansal N K. Effect of moisture transfer across building components on room temperature [J]. *Building and Environment*, 2002, **37**(1): 11 – 17.

[3] Chang W J, Weng C I. Analytical solution to coupled heat and moisture diffusion transfer in porous materials [J]. *International Journal of Heat and Mass Transfer*, 2000, **43**(19): 3621 – 3632.

[4] Cheroto S, Guigon S M S, Ribeiro J W, et al. Integral transform solution of Luikov's equations for heat and mass transfer in capillary porous media [J]. *Drying Technology*, 1997, **15**: 811 – 835.

[5] Pandey R N, Pandey S K, Ribeiro J W. Complete and satisfactory solutions of Luikov equations of heat and moisture transport in a spherical capillary-porous body [J]. *International Communications in Heat and Mass Transfer*, 2000, **27**(7): 975 – 984.

[6] Grasley Z C, Lange D A. Modeling drying shrinkage stress gradients in concrete [J]. *Cement, Concrete and Aggregates*, 2004, **26**(2): 115 – 122.

[7] Bentz D P, Garboczi E J, Quenard D A. Modeling drying shrinkage in reconstructed porous materials: application to

porous vycor glass [J]. *Modeling and Simulation in Materials Science and Engineering*, 1998, **6**(3): 211 - 236.

[8] Grasberger S, Meschke G. A hygro-thermal-poroplastic damage model for durability analyses of concrete structures [C]//*Proceedings of the European Congress on Computational Methods in Applied Sciences and Engineering*. Barcelona, 2000: 1 - 19.

[9] Han M Y, Lytton R L. Theoretical prediction of drying shrinkage of concrete [J]. *Journal of Materials in Civil Engineering*, 1995, **7**(4): 204 - 207.

基于多孔介质湿热迁移的混凝土收缩数值模拟

陈德鹏　　钱春香

(东南大学材料科学与工程学院,南京 211189)

摘要:为了对处于环境温、湿度中的混凝土的收缩变形进行有效数值模拟分析,提出了一种数值解析与有限元分析相结合的方法.根据多孔介质热质传输原理描述混凝土中湿热迁移过程的耦合偏微分方程组,借助 Laplace 变换及传递函数将其简化为拉氏域内的简单微分方程并求解,然后通过 Laplace 逆变换得到物理空间内的温度和含湿量.在此基础上利用有限元分析方法得到混凝土湿热耦合收缩变形.该方法克服了其他求解过程中特征值复杂、耦合困难及准确性差的问题,并有效解决了现有有限元软件难以处理湿度应力及变形的难题.以 Hundt 试验为算例的数值计算表明,模拟结果与试验数据具有良好的相关性.

关键词:耦合湿热迁移;混凝土收缩;数值解析法;传递函数

中图分类号:TU528.01